90

AECL-9510

CFFTP-G-87024

ATOMIC ENERGY OF CANADA LIMITED

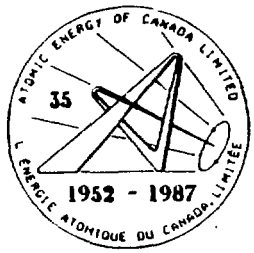

L'ÉNERGIE ATOMIQUE DU CANADA LIMITÉE

FUSION BREEDER SPHERE–PAC BLANKET DESIGN

ENVELOPPE DE RÉGÉNERATION DE RÉACTEURS SURGÉNÉRATEURS À FUSION

J.D. SULLIVAN and B.J.F. PALMER

Chalk River Nuclear Laboratories

Laboratories Nucleaire de Chalk River

Chalk River, Ontario

November 1987 novembre

ATOMIC ENERGY OF CANADA LIMITED

FUSION BREEDER SPHERE-PAC BLANKET DESIGN*

by

J.D. Sullivan and B.J.F. Palmer

*Work funded by Atomic Energy of Canada Limited Research Company and Canadian Fusion Fuels Technology Project

Fuel Materials Branch
Chalk River Nuclear Laboratories
Chalk River, Ontario KOJ 1JO

1987 November

AECL-9510
CFFTP-G-87024

L'ÉNERGIE ATOMIQUE DU CANADA, LIMITÉE

ENVELOPPE DE RÉGÉNÉRATION DE RÉACTEURS SURGÉNÉRATEURS À FUSION

J.D. Sullivan et B.J.F. Palmer

RESUMÉ

Des travaux considérables, dans le monde entier, sont actuellement orientés vers la production de matériaux pour les réacteurs à fusion. De nombreuses usines de céramiques sont engagées dans la fabrication des céramiques au lithium sous diverses formes pour les incorporer à l'enveloppe de régénération de tritium qui entourera le réacteur de fusion. Les enveloppes actuelles comporte de la céramique sous les formes de lit en un seul bloc ou de lit de billes tassées. L'orientation principale à l'EACL est vers la production de billes d'aluminate de lithium à incorporer à un lit de billes tassées. Les études contemporaines de l'enveloppe de régénération apportent une connaissance rudimentaire quant au diamètre de sphères nécessaire. Dans la présente étude, on a examiné les paramètres qui déterminent les propriétés quant à la perte de charge et le caloporteur nécessaires. On a établi qu'un lit de billes optimalisé comporterait deux diamètres de billes: 75% en poids pour un diamètre de 3 mm et 25% en poids pour un diamètre de 0,3 mm.

Combustibles
Laboratoire Nucléaire de Chalk River
Chalk River, Ontario K0J 1J0
1987 novembre

AECL-9510
CEETR-G-8702

ATOMIC ENERGY OF CANADA LIMITED

FUSION BREEDER SPHERE-PAC BLANKET DESIGN

J.D. Sullivan and B.J.F. Palmer

ABSTRACT

There is a considerable world-wide effort directed toward the production of materials for fusion reactors. Many ceramic fabrication groups are working on making lithium ceramics in a variety of forms, to be incorporated into the tritium breeding blanket which will surround the fusion reactor. Current blanket designs include ceramic in either monolithic or packed sphere bed (sphere-pac) forms. The major thrust at AECL is the production of lithium aluminate spheres to be incorporated in a sphere-pac bed. Contemporary studies on breeder blanket design offer little insight into the requirements on the sizes of the spheres. This study examined the parameters which determine the properties of pressure drop and coolant requirements. It was determined that an optimised sphere-pac bed would be composed of two diameters of spheres: 75 weight % at 3 mm and 25 weight % at 0.3 mm.

Fuel Materials Branch
Chalk River Nuclear Laboratories
Chalk River, Ontario K0J 1J0

1987 November

AECL-9510
CFFTP-G-87024

FUSION BREEDER SPHERE-PAC BLANKET DESIGN

J.D. Sullivan and B.J.F. Palmer

1. Introduction

As part of AECL's contribution to the Canadian Breeder Blanket program, lithium-bearing ceramic materials are being developed at CRNL as fuel for fusion reactors. The current thrust is in the development of ceramic spheres to be used in the breeder blanket around the fusion reactor. Current literature does not adequately discuss the required properties of these spheres. This report details a set of calculations carried out to determine the requirements on sphere properties for use in breeder blankets.

2. Background

The first generation of fusion reactors will extract energy from the fusion of deuterium (D) and tritium (T) nuclei to form helium (He) plus a neutron (n) along with 169×10^9 joules per gram of reactants. The ignition temperature for this reaction is 77×10^6 K. The next most likely reaction is the fusion of two deuterons to form tritium plus a proton and 40×10^9 joules per gram of reactant with an ignition temperature of 386×10^6 K. As a result of this much higher ignition temperature, the D-D reaction is much more difficult to achieve, and the D-T reaction is expected to dominate in the production of fusion power.

One problem with the D-T reaction is that tritium is not a naturally occurring isotope, since it decays into ^{3}He plus an electron with a half-life of approximately 12.4 years. Small amounts of tritium are produced in fission reactors, but not in sufficient quantities to satisfy the requirements for fusion reactors. The most likely method for the production of tritium is in the fusion reactor itself. One of the products of the D-T reaction is neutrons and these can be used to produce tritium by the reaction ^{6}Li(n,α)T. To make use of this reaction, most fusion reactor designs have the reactants surrounded with lithium-containing materials. The portion of the reactor which absorbs neutrons to produce tritium plus useful thermal energy, is called the breeder blanket.

There are many different forms that a fusion reactor may take. That shown in Figure 1 has the reactants in the form of a plasma which is magnetically constrained to travel around a torus. This design of reactor is called a tokamak. Other designs have the plasma moving along a linear channel with magnetic mirrors at the ends of the channel to contain the plasma. These are tandem mirror reactors. Not all designs have a plasma as the fuel. In one favoured design, the tritium is contained in small glass capsules which are imploded by converging laser beams. The process is called inertial confinement and the conditions for fusion are achieved during the implosion. The calculations in this report are not based on a specific design but are intended to assess the criteria for a blanket which may be found in many reactors.

The material containing the lithium can be in many forms including molten lithium metal, lithium-lead eutectic (17Li-83Pb), molten lithium fluoride salt or lithium-containing ceramics. The hypothetical blanket in these calculations has a ceramic breeder. Some properties of a number of candidate ceramic breeder materials are listed in Table I, along with those of lithium metal. A major advantage of ceramic materials is their ability to withstand high temperatures and remain in the solid state. Many lithium ceramics have lithium concentrations comparable to, or even higher than, solid lithium metal.

Chemical and physical properties of a number of candidate ceramic breeder materials are listed in Table II. This study concentrates on γ-lithium aluminate because of its chemical and thermal stability.

Just as there are many designs of reactors, there are also many different designs for the blanket. In most, the breeder is contained in blanket segments, called modules. The modules are arranged around the outside of the reactor to form the blanket. Two forms of modules are shown in Figures 2 and 3. The design in Figure 2 has the breeder in the form of solid slabs (monoliths) and Figure 3 has a bed of packed spheres (sphere-pac). Some designs have sphere-pac beds in the form of slabs [1], but it will be shown in this report that such a design is not practical.

There are a number of advantages to sphere-pac blanket designs, including:

- bed thermal conductivity is dominated by the gas phase, so the effects of irradiation on bed thermal conductivity are small,

- bed thermal conductivity can be varied (by varying purge gas pressure) allowing control over temperature distributions as reactor power is changed,

- there is no thermal stress cracking in the ceramic because temperature gradients across the spheres are small (sintered slabs will have large thermal stresses), and

- thermal contact with cooling tubes is maintained during irradiation-induced swelling and other blanket disruptions.

A sphere-pac blanket, as pictured in Figure 3, has been assumed in these calculations. The portion of the module near the first wall is predominantly beryllium (primarily for neutron multiplication), with a small ceramic component. The heat load in this region is very large. This portion of the blanket can be regarded as separate from the breeder region and is not considered here.

The goals of this study were to assess the feasibility of the helium cooled sphere-pac bed design and to determine the required properties of the spheres that make up the bed. The thermal loads and temperature profiles used in this study were taken from a water cooled study [2], so either water or helium could be used in this design.

3. Design Criteria

One of the goals of this study was to determine the range of sphere sizes required for a sphere-pac breeder blanket. This was done by carefully examining blanket design criteria, including:

- sphere-pac bed thermal conductivity,
- purge gas pressure
- thermal gradients in blanket (ie. cooling tube separation),
- thermal gradients and pressure drop in cooling gas, and
- thermal and stress gradients in spheres.

The choice of parameters is design specific and, to some extent, arbitrary. The procedure followed in this design study was to choose parameters typical of a breeder blanket [1,2] and to ensure that the various aspects of the design were self-consistent. After several iterations, the following blanket parameters were chosen for this study:

Ceramic	Lithium Aluminate
Thermal Loading	10 W/cm^3 (varies throughout blanket)
Coolant	Helium at 5 MPa flowing at 50 m/s
Cooling System	1 cm diameter tubes through bed
Purge Gas	Helium at 0.1 MPa (nominal)
Purge Gas Flow Rate	15 m^3/s
Blanket Volume	300 m^3
Blanket Porosity	17%
Blanket Temperature	700 K (nominal varies throughout blanket)

Since one of the goals of this study was to determine the sizes of spheres required, many of the properties calculated in this report are expressed as a function of sphere size.

4. Sphere Packing

One of the requirements of making a sphere-pac bed is an understanding of how spheres can be packed into a volume. Since the properties of the sphere-pac bed must be well known and controlled, the calculations here have assumed a vibratory compacted bed of spheres of well known size and size distribution.

A mass of mono-sized spheres can be vibratory packed to a density of approximately 63% of theoretical density (in this case, theoretical density is the density of the spheres) in a container of dimensions at least ten times the sphere diameter [3]. This result has been found for containers with both square and circular cross section and is thus not crucially dependent on container shape. The density can be further increased by adding a second fraction of mono-sized spheres of smaller diameter which fits into the spaces between the larger spheres. The density of the combined spheres approaches 83% of theoretical if the diameter of the smaller size fraction is one seventh that of the larger size fraction. A third size fraction one seventh the diameter of the second can yield a density of approximately 90%. As the number of size fractions raises, the

difficulty of compaction increases, since the number of spheres being added increases very rapidly (number of spheres is proportional to (mass/diameter^3). Fabrication of the smaller fractions becomes a problem because of the need to produce large numbers of spheres. There is also an increase in the sphere-sphere interaction as the size of the spheres is reduced.

In order that the design be conservative, it has been assumed that the size requirements on the spheres are that the diameter of the largest spheres be one tenth of the size of the cavity being filled, and that subsequent size fractions have diameters one tenth of the previous fraction.

5. Thermal Conductivity

Original attempts to calculate thermal conductivities of sphere-pac beds considered only the bulk properties of the constituents of the bed (solid spheres and fill gas) [4]. Subsequent calculations have included the effects of mean free path of the gas molecules and radiant heat transfer between the spheres [5]. The method used is briefly described below. It was found that the effects of radiation on bed thermal conductivity are negligible for any bed considered here, so the simpler formulae including only mean free path effects are described here.

The procedure is to calculate the thermal conductivities of two reference systems, specifically a cubic array of spheres and a cubic array of cylinders. The densities of both (theoretical) systems are known exactly; the cubic-packed sphere system has a density of 52.4%, and the cubic array of cylinders 78.5%. The results of these calculations, along with the properties of the constituent materials (spheres and gas phase) are used in a logarithmic interpolation procedure to calculate the properties of a bed of arbitrary density.

The thermal conductivity of a cubic-packed bed of mono-sized spheres is given by

$$k = \frac{\pi}{2\,(\delta - 1)^2}\left[\delta - 1 - (1+m)\ln\left(\frac{\delta + m}{1+m}\right)\right] + 1 - \frac{\pi}{4} \qquad (1)$$

where $k = k_b/k_g$ is the ratio of bed thermal conductivity (k_b) to gas phase conductivity (k_g),

$\delta = k_g/k_s$ is the ratio of gas phase conductivity to sphere conductivity (k_s), and

$m = g/D$ is the ratio of jump distance (g) to sphere diameter (D).

The thermal conductivity of a cubic array of cylinders is given by:

$$k = \frac{1+m}{1-\delta} \; \frac{\pi - 2\sin^{-1}\left[\left(\frac{\delta+m}{2(1+m)}\right)^{1/2}\right]}{\left[(\delta+m)(2-\delta+m)\right]^{1/2}} - \frac{\pi}{2(1-\delta)} \qquad (2)$$

with variables as described above (D is the diameter of the cylinders).

Interpolation of the above results to that for a bed of arbitrary porosity, x, is done using a logarithmic equation of the form

$$y = -\frac{(x-c)(x-d)(x-1)}{c\,d}\,y_0 + \frac{x(x-d)(x-1)}{c(c-d)(c-1)}\,y_c + \frac{x(x-c)(x-1)}{d(d-c)(d-1)}\,y_d + \frac{x(x-c)(x-d)}{(1-c)(1-d)}\,y_1 \qquad (3)$$

where $y=\ln k = \ln k_b/k_g$ yields the thermal conductivity for the bed of porosity x, and the subscripts 0, c, d and 1 refer to systems of porosity 0 (ie solid), $c=1-\pi/6=0.476$ (cubic-packed spheres), $d=1-\pi/4=0.215$ (cubic array of cylinders) and 1 (gas phase). In each case $y_i=\ln k_i/k_g$.

Notice that the thermal conductivity of a sphere-pac bed, k_b, is calculated relative to the gas thermal conductivity, k_g. This emphasizes the importance of the gas phase to the thermal conductivity of the bed. There is only point contact between adjacent spheres in the bed, so although the solid has a higher conductivity, it is the gas phase (the continuous phase in the bed) which controls heat flow. If sintering causes the formation of necks between the spheres, the above results must be altered, since the conductivity of the bed will increase.

The properties of the bed are a function not only of the sphere diameters, but also of the number of fractions making up the bed. For beds composed of more than one fraction of mono-sized spheres, an effective diameter is used in the above equations. If there are n size fractions, and the i^{th} fraction has diameter D_i and mass fraction m_i, then the effective diameter is

$$D = \frac{\sum_{i=1}^{n} m_i^{1/3}}{\sum_{i=1}^{n} \frac{m_i^{1/3}}{D_i}} \qquad (4)$$

Thus the necessary input parameters for the calculation of the thermal conductivity of a sphere-pac bed are:

- sphere sizes,
- number of size fractions,
- ceramic thermal conductivity,
- purge gas thermal conductivity, and
- purge gas jump distance.

The thermal conductivity of γ-lithium aluminate is 2.4 W/m K (given by 1.47 + 943/T [6]). Helium gas at 0.1 MPa has a thermal conductivity of 0.268 W/m K (given by .003366 x $T^{0.668}$ [7]). The jump distance, g, is related to the mean free path of atoms in the gas. At 700 K and 0.1 MPa, helium has a jump distance of 10 μm, and nitrogen 0.75 μm [5]. The bed thermal conductivity was calculated as a function of maximum sphere size for beds containing one-, two- and three-fraction mixtures and is shown in Figure 4.

The solid has a higher thermal conductivity than the purge gas, so higher densities are generally favoured. The size of the gaps between the spheres controls the efficiency of heat transport in the purge gas and if these gaps are comparable in size to the jump distance of the gas, thermal transport is impeded. This effect can be seen in the bed thermal conductivities, especially for three-fraction beds, in which the spacing between the smaller spheres is of the order of the jump distance. This again emphasizes the importance of the purge gas to the bed conductivity.

For the size range of interest (maximum sphere diameter between 1 and 3 mm in most designs), a two-fraction bed has a higher thermal conductivity than a three-fraction bed, even though a three-fraction bed has a higher solid packing density. In this size range, it is a combination of packing density and minimum sphere size that determines thermal conductivity.

6. Purge Gas Pressure Drop

Tritium is produced in the breeder material and must be collected to be used as fuel for the reactor. The process for doing this involves the use of a purge gas that flushes tritium out of the solid breeder and into a concentration and collection facility. Tritium production rates and inventories are known [1,2] and it has been estimated that the purge gas replaces the gas in the blanket every three seconds. This forms the necessary input for a calculation of purge gas pressure drop.

The purge gas used in this calculation was helium at ambient (one atmosphere) pressure [2]. Some studies have this gas at ten atmospheres (1 MPa) [1]. This higher pressure increases the thermal conductivity of the blanket, reducing thermal gradients. The calculations in this study are meant to be conservative, so only the one atmosphere design is considered here. The pressure drop is calculated using expressions for an incompressible gas flowing through a bed of spheres [8]. (Although the gas is actually compressible, the effects of compressibility on the pressure drop were found to be negligible.) To simplify the calculation, the blanket module is assumed to be in the form of a block of dimensions 0.3 x 0.3 x 2 m. The purge gas flows in the long direction through the block.

The pressure drop, δP, in the purge gas is given by the expression [8]

$$\delta P = \frac{2\, f_m\, G^2\, L\, (1 - x)^{3-n}}{D_p\, d\, \emptyset_s{}^{3-n}\, x^3} \tag{5}$$

where f_m is a friction number, which is a function of the modified Reynolds number $N_{Re}' = D_p\, G/\mu$ (in these calculations, f_m is given by $\log(f_m) = -\log(N_{Re}') + 2$)
D_p is the sphere diameter,
G is the superficial mass velocity (weight rate of flow divided by total cross sectional area, ignoring that portion of the area occupied by spheres),
μ is the gas viscosity,
L is the length of the bed,
d is the gas density,
$\emptyset_s$ is a shape factor ($\emptyset_s = 1$ for spheres), and
x is the pore fraction.
n is a function of the modified Reynolds number and, in this case, $n \sim 0$

For the case in which there are N size fractions in the bed, the effective sphere diameter is given by [8]

$$D_p = \left[\sum_{i=1}^{N} \frac{m_i}{D_{pi}} \right]^{-1} \tag{6}$$

where m_i is the mass fraction of size fraction i and
D_{pi} is the diameter of fraction i.

Notice that this expression for effective diameter is different from that used in the thermal conductivity calculation.

The viscosity of helium used in these calculations was $\mu = 3.7 \times 10^{-5}$ kg m^2/s and the density was 6×10^{-2} kg/m^3. The pressure drop as a function of maximum sphere size for one-, two- and three-fraction beds is shown in Figure 5. As was the case with thermal conductivity, it can be seen that it is the smallest sphere size which controls pressure drop since for a given maximum sphere size the largest pressure drop occurs in beds

containing the smallest size fraction. Larger size spheres are clearly favoured if the pressure drop is to be minimized. For a given maximum sphere diameter, it is preferable to have fewer size fractions to reduce the pressure drop. The pressure drop, in a two-fraction bed of spheres in which the larger size is 3 mm diameter, is approximately 0.25 MPa. Given that this is a scoping calculation to determine the requirements on sphere size for the breeder blanket, a pressure drop of 0.25 MPa can be regarded as acceptable, even though the ambient pressure is only 0.1 MPa. Small design refinements (increasing the purge gas inlet pressure to 0.35 MPa for example) can compensate for this pressure drop.

It has been suggested that the design in Figure 2 be used for a sphere-pac bed [1]. The idea is to form slabs of spheres bound in a casing. The purge gas is to flow in the slab in the direction of the longest dimension. The sphere-pac bed is to be composed of 1200 μm (59 wt%), 300 μm (20 wt%) and 30 μm (21 wt%) diameter spheres [1,9]. The purge gas back pressure for this case would be 4500 psi (30 MPa). This is much greater than the ambient purge gas pressure of 0.1 MPa (or the proposed pressure of 1.0 MPa [1]) and can be regarded as impractical if no alternative purge flow path is provided. In this flow regime, the pressure drop is approximately proportional to flow rate, so even decreasing the flow rate by an order of magnitude would only reduce the pressure drop to 3 MPa (450 psi).

7. Thermal Gradients in Blanket

An important constraint in the design criteria for sphere-pac beds (see Figure 3) is the spacing between the coolant tubes (in the plate design, Figure 2, this corresponds to the plate thickness). If the spheres are to pack to the required density, the spaces between the tubes must be approximately ten times the diameter of the largest size fraction of spheres. The tube spacing is determined by the temperature profile in the bed, which is determined by the bed conductivity (a function of sphere sizes) and the local thermal load. Thus the problem is convoluted and must be solved iteratively by:

- calculating a temperature profile based on assumed sphere sizes,

- determining the tube spacing required to keep the maximum blanket temperature within limits,

- determining whether the spheres will fit into the resultant inter-tube spaces, and if not,

- choosing a more appropriate set of sphere sizes and repeating the calculation.

The tube spacings in this section have been calculated for the sphere-pac bed containing two fractions of spheres, one 3 mm diameter and the other 300 μm diameter.

Some previous attempts to determine coolant tube spacings have used the assumption that each tube extracts heat from a cylindrical region of

blanket centred on the tube, and have required that all portions of the blanket be contained within one of these cylinders. This approximation clearly overcools the blanket (see Figure 6a). A better approximation is to assume that each tube cools a block of blanket (of side 2a, see Figure 6b) and that these blocks adjoin one another, but do not overlap. The temperature distribution is calculated by using a quadrupolar solution to the heat flow equation. The maximum temperature in the bed is given by [10]

$$T_{max} - T_{min} = \frac{qa^2}{4k} \left[(b/a)^2 - 1.219 \ln((b/a)^2) - 0.765 \right] \quad (7)$$

where T_{max} is the maximum temperature in the block being cooled by the tube (found at a corner of the block),
T_{min} is the minimum temperature in the block (found adjacent to the cooling tube),
q is the thermal load,
k is the thermal conductivity of the bed,
$2b$ is the diameter of the cooling tube, and
$2a$ is the length of the side of the block.

This solution has the property of having a temperature derivative of zero at angles of $\pi/16$, $\pi/4$ and all symmetrical reflections of these angles around the square end of the block being cooled. The maximum temperature in the blanket is shown in Figure 7 for both a sphere-pac bed (k=1.4 W/m K) and a monolithic slab (k=2.4 W/m K) as a function of tube gap (spacing between the surfaces of the tubes) for 1 cm diameter cooling tubes. In this figure it can be seen that the temperatures in a sphere-pac bed are not significantly greater than those in a monolithic blanket.

The thermal load used was q=5 W/cm^3. The actual thermal load expected in the sphere-pac bed [2] varies from 20 W/cm^3 in the region close to the first wall of the module, down to approximately 3 W/cm^3 close to the back wall. The length of the ceramic portion of the blanket in which the thermal load exceeds 10 W/cm^3 is less than 3 cm, and the length over which it exceeds 5 W/cm^3 is approximately 5 cm. The rest of the ceramic portion of the blanket has a thermal load of less than 5 W/cm^3. The maximum temperature in the blanket is linear in q (see above equation) making calculations of tube spacings for various thermal loads straightforward. The maximum blanket temperature is within 500°C of the coolant tube temperature for a coolant tube spacing (surface-to-surface) of 1.5 cm, equivalent to a centre-to-centre spacing of 2.5 cm, for a thermal load of 10 W/cm^3. For most of the blanket the tube spacing can be larger.

8. Thermal Gradients and Pressure Drop in Cooling Gas

The coolant flowing in the tubes (see Figure 3) can be either water or helium. Some lithium ceramics react with water (ie. Li_2O) and, for this reason, water is considered to be a less desirable coolant. The following calculations have been carried out assuming helium as the coolant. The thermal loads and temperature distributions used in these calculations have been taken from a water cooled design [2], so this design would be compatible with water cooling.

To increase the density of the coolant, and thus the volumetric heat capacity, the coolant is under 5 MPa pressure. The calculated quantities are:

- change in bulk coolant temperature,
- change in temperature across the breeder/coolant interface, and
- pressure drop along the coolant tube.

The increase in temperature (δT) of the bulk coolant is calculated using the equation

$$\delta T = \frac{4a^2 q}{\pi b^2 d_c C_p v} \tag{8}$$

where q is the (steady state) heat load
d_c is the coolant density
C_p is the coolant heat capacity
v is the coolant velocity, and
a,b are defined above.

The change in temperature per unit length was calculated for q = 5 and 10 W/cm^3 as a function of coolant velocity, and is shown in Figures 8 and 9.

The breeder blanket is composed of spheres and purge gas, both of which are in intimate contact with the coolant tubes (this is one of the beneficial aspects of this design). Thus there is no temperature drop across the breeder/coolant tube interface. The thermal conductivity of the coolant tube is considerably higher than that of the sphere-pac bed, so the temperature drop across the tube wall is negligible. This leaves only the temperature drop across the tube/coolant interface, which was calculated using the Sieder-Tate equation for forced convection heat transfer to turbulent flow in circular tubes [8]

$$N_{Nu} = 0.023\, N_{Re}^{0.8}\, N_{Pr}^{1/3}\, (\mu_b/\mu_w)^{0.14} \tag{9}$$

where
N_{Nu} =hd/k is the Nusselt Number,
h is the heat transfer coefficient,
d is the tube diameter,
k is the coolant thermal conductivity,

N_{Re} is the Reynolds Number,
N_{Pr} is the Prandtl Number, and
μ_b, μ_w are the coolant viscosities at the bulk and wall temperatures.

In these calculations the variation in viscosity at bulk and wall temperatures has been ignored. This equation is solved for h and substituted into

$$q = h\ A\ \delta T \tag{10}$$

where A is the surface area of the tube. Plots of the interface temperature differences as a function of coolant velocity are also shown in Figures 8 and 9.

An examination of Figure 9 shows that for a coolant velocity of 50 m/s, at a thermal load of 10 W/cm^3, the increase in coolant temperature is less than 120 K and the interface δT is less than 80 K. Thus the maximum temperature of the breeder adjacent to a coolant tube is less than 200 K greater than the coolant inlet temperature.

The pressure drop per unit length ($\delta P/L$) in the coolant gas was calculated using the expression [8]

$$\frac{\delta P}{L} \sim 0.5\ v^2\ D\ (\ f/d\ ) \tag{11}$$

where v is the coolant velocity,
D is the coolant density,
d is the tube diameter, and
f is a Fanning Factor, which is a function of the Reynolds Number.

Over the range of Reynolds Numbers encountered in these calculations ($10{,}000 < N_{Re} < 90{,}000$), f is approximately given by

$$f \sim 0.06737 - 0.0095 \log(\ N_{Re}\ ). \tag{12}$$

A plot of pressure drop as a function of coolant velocity is shown in Figure 10. For a coolant velocity of 50 m/s, the pressure drop is 10 kPa. This is insignificant when compared to the coolant pressure of 5 MPa.

9. Thermal and Stress Gradients in Spheres

The temperature difference between the centre of a sphere (Tmax) and its surface (Tmin) is egiven by [11]

$$T_{max} - T_{min} = \frac{q\, d^2}{24\, k} \tag{13}$$

where q is the heat load,
d is the sphere diameter, and
k is the thermal conductivity.

The maximum thermal stress (σ) is given by [11]

$$\sigma = \frac{2}{5} \frac{E\, \alpha}{1-\mu} (T_{max} - T_{min}) \tag{14}$$

where E is Youngs Modulus,
α is the coefficient of thermal expansion, and
μ is Poisson's ratio.

The values used were E = 230 GPa, $\alpha = 1.2 \times 10^{-5} K^{-1}$ and $\mu = 0.23$. A plot of Tmax - Tmin and σ as a function of sphere diameter for a heat load of 10 W/cm^3 is shown in Figure 11.

For 3 mm diameter spheres, the central temperature can be expected to be less than 2°C greater than the surface temperature and thermal stresses less than 5 MPa. The fracture stress for lithium aluminate is approximately 70 MPa, so thermal stress cracking is not expected in the spheres.

In a 1 cm thick monolithic slab of lithium aluminate under a thermal load of 10 W/cm^3, the central temperature is given by [11]

$$T_{max} - T_{min} = \frac{q\, \delta^2}{2\, k} \tag{15}$$

where δ is the slab thickness, and the thermal stress is [11]

$$\sigma = \frac{1}{6} \frac{E\, \alpha}{1-\mu} (T_{max} - T_{min}) \tag{16}$$

with variables as above. Under the conditions δ = 1 cm and q = 10 w/cm^3, the central temperature exceeds the surface temperature by 50°C and the thermal stress is 155 MPa. Central melting is not expected, but in regions of high thermal load (10 W/cm^3), cracking seems likely. Sphere-pac beds are much less likely to experience thermal cracking than are monolithic blankets.

10. Conclusions

As a result of this investigation, it was concluded that the optimum blanket performance will be obtained in a blanket composed of two sizes of spheres: 75 weight percent 3 mm diameter and 25 weight percent 0.3 mm diameter. The bed can be cooled efficiently using flowing helium in pressurized tubes distributed throughout the bed, and sufficient purge gas can be swept through the bed to recover tritium for fueling of the reactor. Either helium or water can be used to cool the blanket.

With a tube gap of 1.5 cm (2.5 cm centre-to-centre), the maximum blanket temperature exceeds the coolant temperature by 500°C or less. With helium as the coolant, flowing at 50 m/s along 1 cm diameter tubes of length 1 m, the maximum temperature of the breeder, adjacent to the coolant tube, is 200°C greater than the coolant inlet temperature. If the coolant inlet temperature is 250°C, then the maximum breeder temperature adjacent to a coolant tube is 450°C, and thus the maximum breeder temperature does not exceed 950°C, and is, on average, considerably less than this. The pressure required to flow the coolant through the pipes is insignificant, and the pressure required to flow the purge gas through the bed is not excessive. There should be no thermal stress cracking of the ceramic, and no instances of local melting. The details of tritium production, migration and recovery have not been addressed in this report, and this aspect of the design should be considered. Also, no consideration is given here for the high thermal load neutron multiplier region near the first wall.

11. Acknowledgements

The authors thank Dr. W. Selander for calculating the quadrupole solution to the heat flow equation, Dr. G.R. Dimmick for discussions on cooling gas pressure and heat flow calculations, and Drs. P. Gierszewski of CFFTP and A.R. Raffrey of U.C.L.A. for helpful discussions.

12. References

[1] M.A. Abdou, et al, "FNT Progress Report: Modelling & FINESSE", Report UCLA-ENG-86-44, January, 1987.

[2] D.L. Smith et al, "Blanket Comparison and Selection Study", Report ANL/FRR-84-1, Argonne National Laboratory, 1984.

[3] R.K. McGeary, "Mechanical Packing of Spherical Particles", J. Am. Ceram. Soc. 44 [10] 513 - 522 (1961).

[4] R.G. Deissler and C.S.Eian, "Investigation of Effective Thermal Conductivities of Powders", US National Advisory Committee for Aeronautics Report NACA RM E52C05, 1952.

[5] R.A.O. Hall and D.G. Martin, "The Thermal Conductivity of Powder Beds...", J. Nucl. Mater. 101 172 - 183 (1981).

[6] G.W. Hollenberg, "Planning Document for FUBR-1B Experiment, Second Insertion", Hanford Engineering Development Laboratory, 1984.

[7] J.M. Gandhi and S.C. Saxena, "Correlated Thermal Conductivity Data of Rare Gases and Their Binary Mixtures at Ordinary Pressures", J. Chem. Eng. Data 13, 3, (1968).

[8] R.H. Perry, D.W. Green and J.O. Maloney, "Perry's Chemical Engineers' Handbook", Sixth Edition, McGraw-Hill, New York, 1984.

[9] J.P. Moore, R.J. Dippenaar, R.O.A. Hall and D.L. McElroy, "Thermal Conductivity of Powders...", Report ORNL/TM-8196, Oak Ridge National Laboratory, 1982.

[10] W.N. Selander, private communication.

[11] R. Hankel, "Stress and Temperature Distributions", Nucleonics 18, No. 11, 168 - 169 (1960).

Table I. Some Candidate Ceramic Solid Breeder Materials

Formula	Name	Density		Melting Temperature (°C)
		Total (g/cm^3)	Lithium (g/cm^3)	
Li_2O	Lithium Oxide	2.01	0.94	1433
$LiAlO_2$	γ-Lithium Aluminate	2.55	0.27	1610
Li_2SiO_3	Lithium Metasilicate	2.52	0.39	1200
Li_4SiO_4	Lithium Orthosilicate	2.21	0.51	1255*
Li_2ZrO_3	Lithium Metazirconate	4.15	0.38	1500
Li_2TiO_3	β-Lithium Metatitanate	3.43	0.43	1540
Li	Lithium (metal)	0.534	0.534	180.5 B.P. 1347

* Decomposes

Table II. Chemical and Physical Properties of Lithium Ceramics

Name	Properties
Lithium Oxide	very hygroscopic, reacts with CO_2, high Li partial pressure, high thermal expansion (2.9% @1000 °C)
γ-Lithium Aluminate	chemically stable, high M.P., low Li partial pressure,
Lithium Metasilicate	fairly low Li partial pressure, low thermal expansion (1.1% @1000 °C)
Lithium Orthosilicate	decomposes at 1255°C rather than melt, reversible phase transformation at 666°C, high thermal expansion (2.7% @1000 °C)
Lithium Metazirconate	phase diagram not known, fairly low Li partial pressure, low thermal expansion (1.0% @1000 °C), reacts with HT-9 alloy to form scale
β-Lithium Metatitanate	if composition altered slightly, forms liquid at 1200°C, slight reaction with 316 SS

LIST OF FIGURES

Figure 1. The STARFIRE tokamak [2], an example of an experimental fusion reactor design.

Figure 2. A blanket module for a helium cooled monolithic breeder reactor [1].

Figure 3. A blanket module for a tube cooled sphere-pac bed breeder [2].

Figure 4. Thermal conductivities of sphere-pac beds. The ceramic is lithium aluminate, the gas permeating the bed is helium at 0.1 MPa and the ambient temperature is 1000 K.

Figure 5. Purge gas pressure drop as a function of maximum sphere size for one-, two- and three- fraction beds.

Figure 6. Approximations to cooling of blanket by tubes.

Figure 7. Temperature extremes in sphere-pac bed and monolithic blankets under a heat load of 5 W/cm^3 and cooled by helium flowing through 1 cm diameter tubes. A quadrupole solution of the heat flow equation has been used.

Figure 8. Change in temperature in the helium cooling gas (per meter of cooling tube) and across the coolant-blanket interface as a function of coolant velocity, for a heat load of 5 W/cm^3.

Figure 9. Change in temperature in the helium cooling gas (per meter of cooling tube) and across the coolant-blanket interface as a function of coolant velocity, for a heat load of 10 W/cm^3.

Figure 10. Coolant pressure drop per unit tube length as a function of coolant velocity.

Figure 11. Maximum thermal stress and temperature extremes in lithium aluminate spheres under a heat load of 10 W/cm^3 as a function of sphere diameter. The fracture strength of lithium aluminate is 73 MPa.

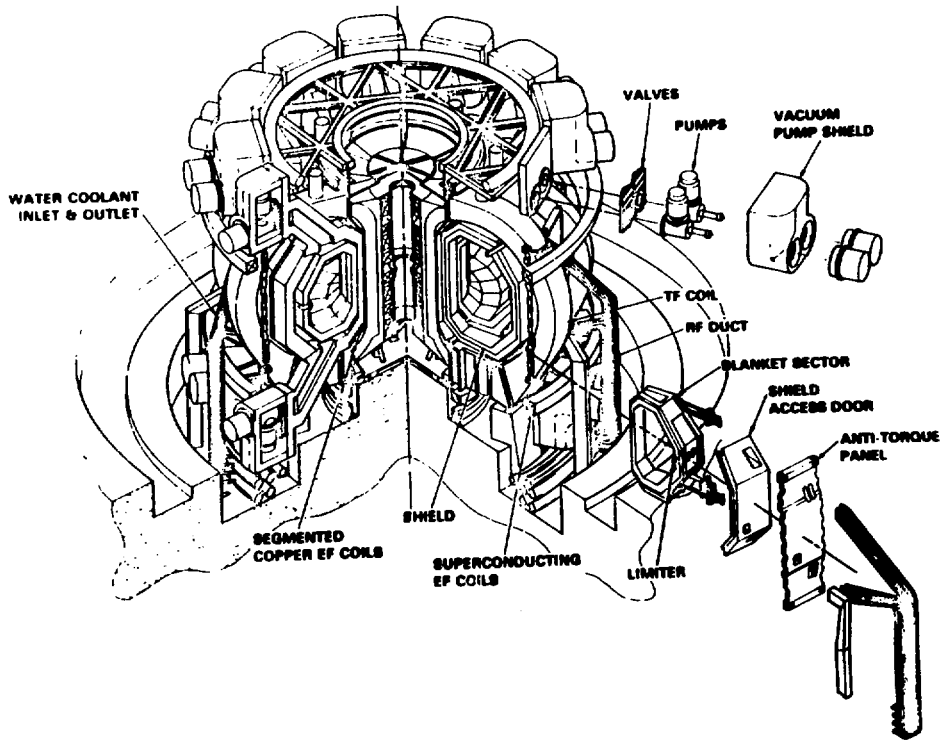

Figure 1. The STARFIRE tokamak [2], an example of a power fusion reactor design.

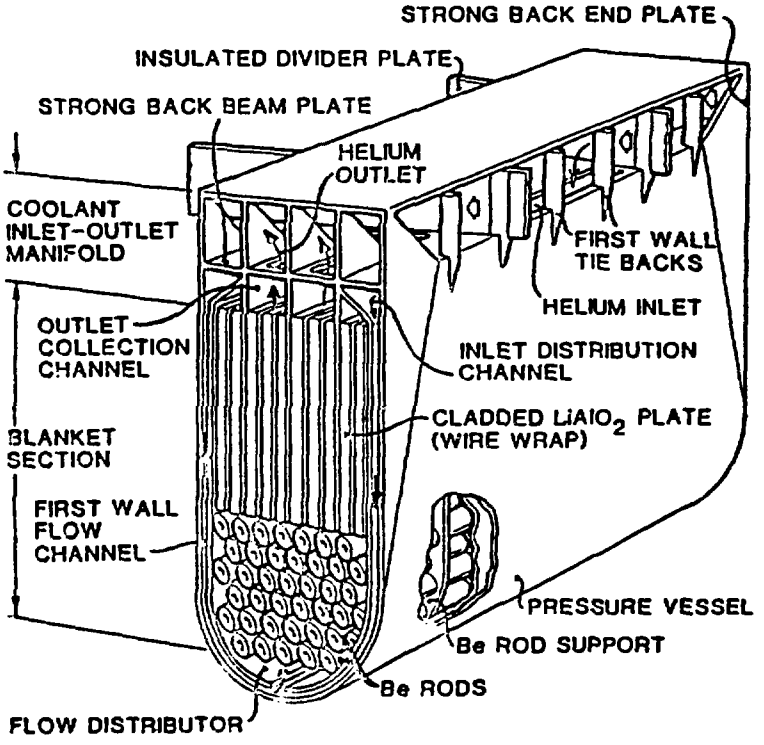

Figure 2. A blanket module for a helium cooled monolithic breeder reactor [2].

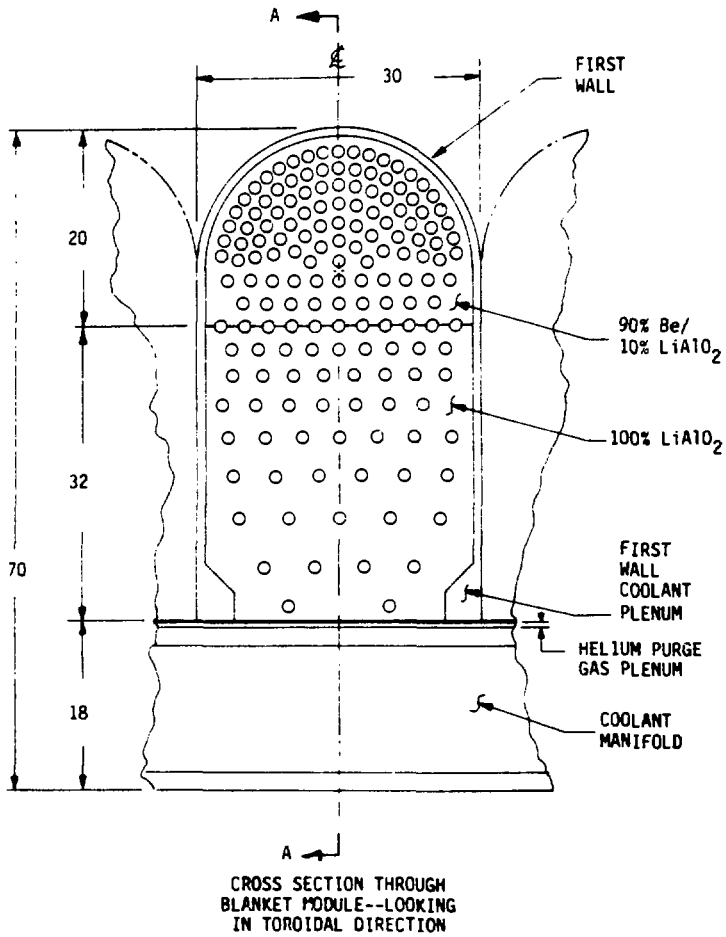

Figure 3. A blanket module for a tube cooled sphere-pac bed breeder [2].

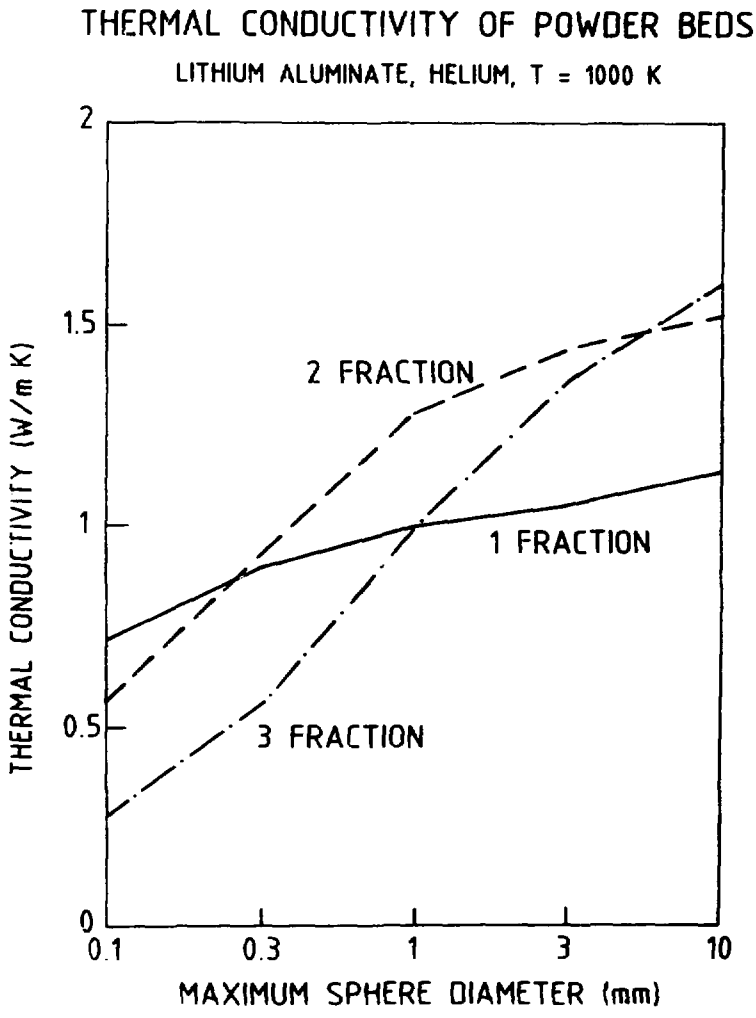

Figure 4. Thermal conductivities of sphere-pac beds. The ceramic is lithium aluminate, the gas permeating the bed is helium at 0.1 MPa and the ambient temperature is 1000 K.

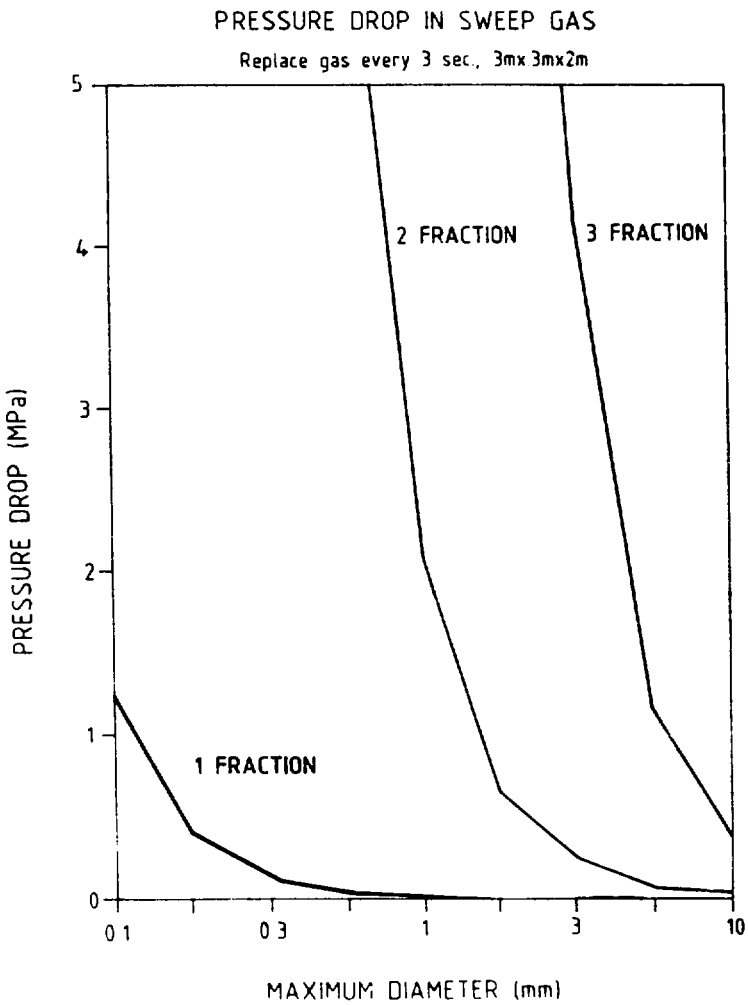

Figure 5. Purge gas pressure drop as a function of maximum sphere size for one-, two- and three- fraction beds.

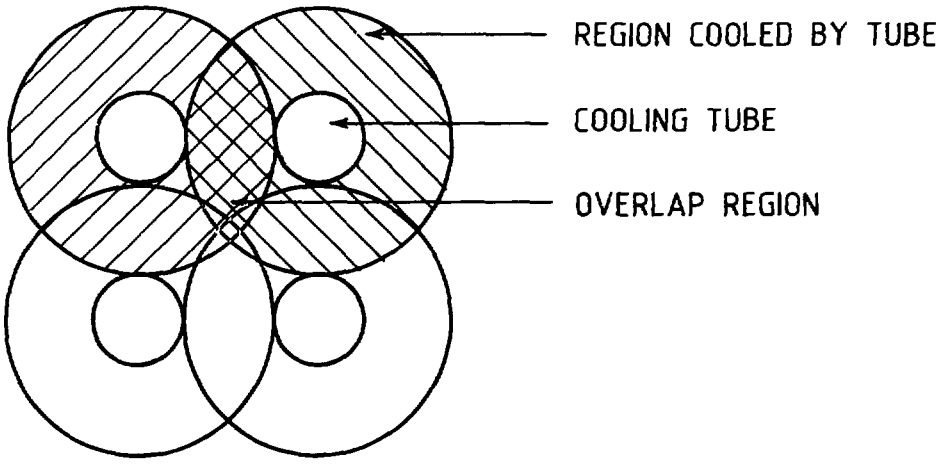

CYLINDRICAL APPROXIMATION TO COOLING

(a)

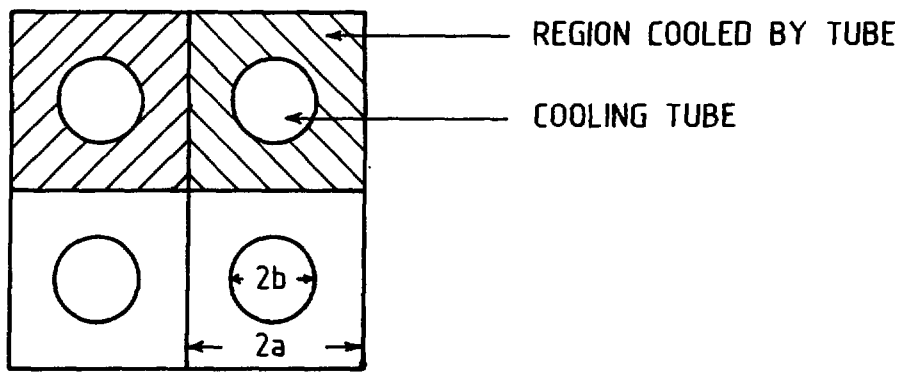

QUADRUPOLE APPROXIMATION TO COOLING

(b)

Figure 6. Approximations to cooling of blanket by tubes.

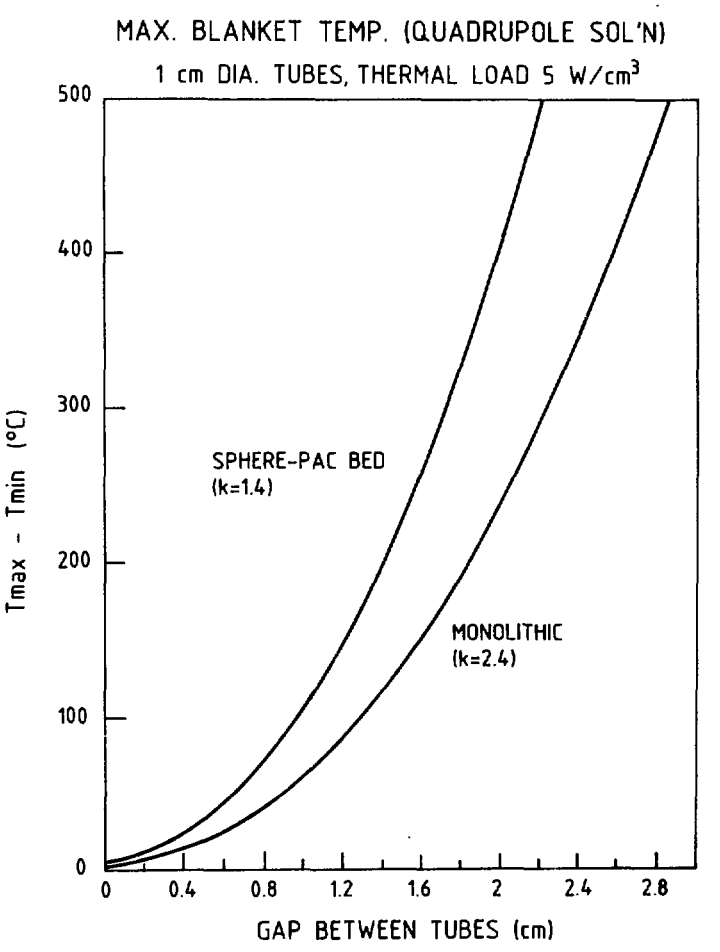

Figure 7. Temperature extremes in sphere-pac bed and monolithic blankets under a heat load of 5 W/cm^3 and cooled by helium flowing through 1 cm diameter tubes. A quadrupole solution of the heat flow equation has been used.

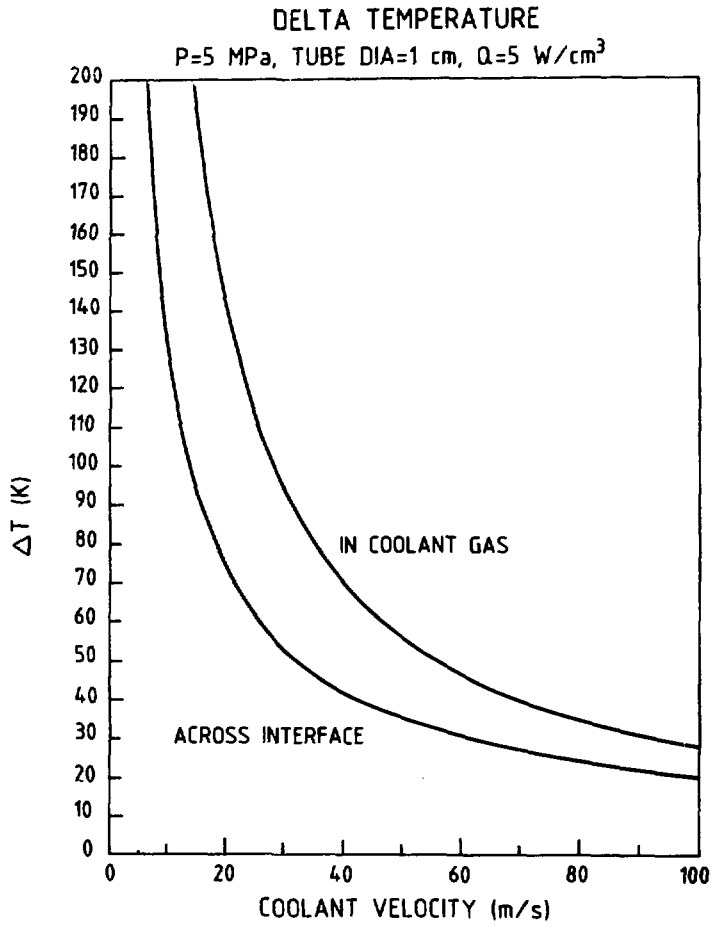

Figure 8. Change in temperature in the helium cooling gas (per meter of cooling tube) and across the coolant-blanket interface as a function of coolant velocity, for a heat load of 5 W/cm^3.

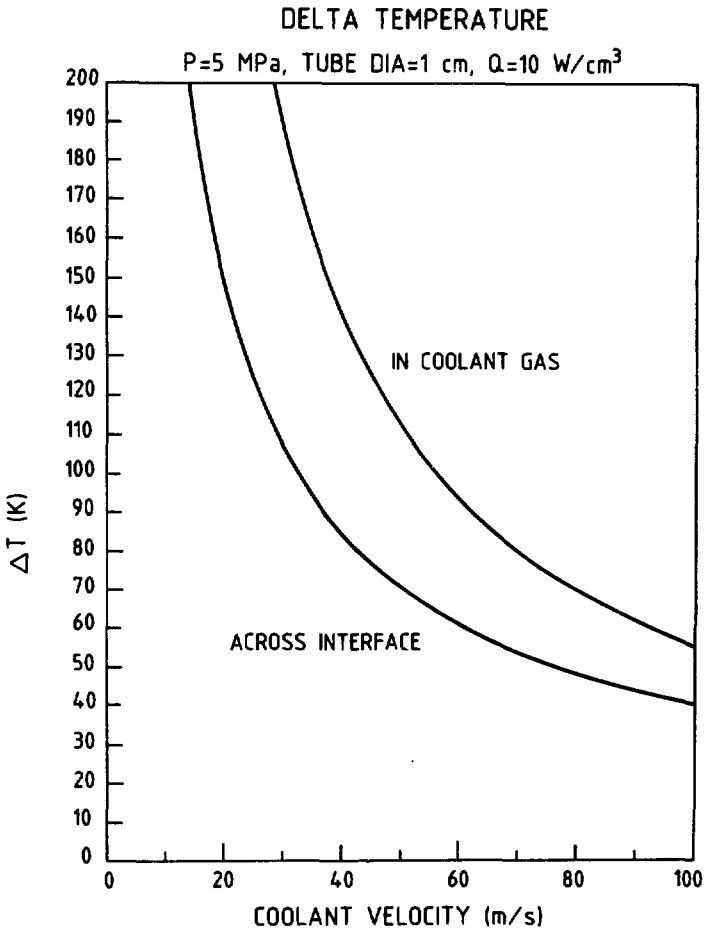

Figure 9. Change in temperature in the helium cooling gas (per meter of cooling tube) and across the coolant-blanket interface as a function of coolant velocity, for a heat load of 10 W/cm^3.

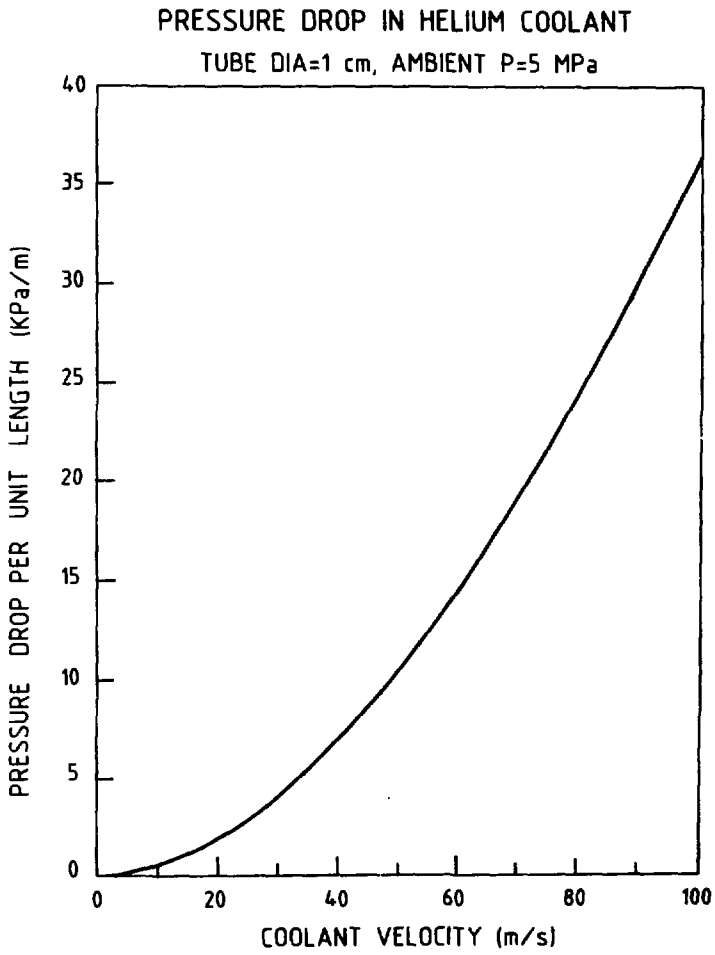

Figure 10. Coolant pressure drop per unit tube length as a function of coolant velocity.

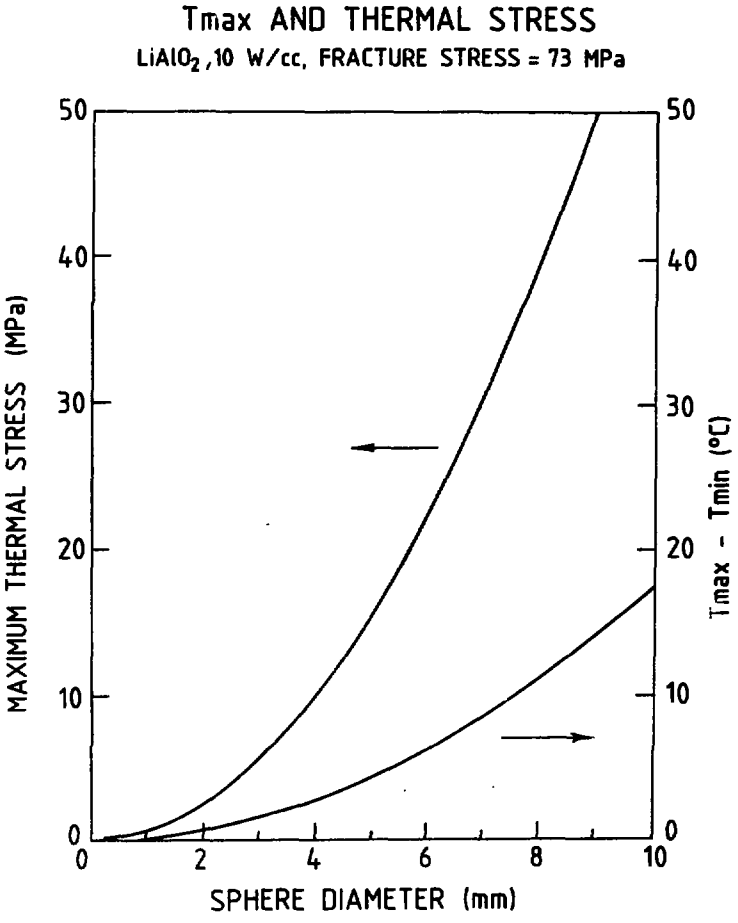

Figure 11. Maximum thermal stress and temperature extremes in lithium aluminate spheres under a heat load of 10 W/cm^3 as a function of sphere diameter. The fracture strength of lithium aluminate is 73 MPa.

ISSN 0067 0367

To identify individual documents in the series we have assigned an AECL- number to each.

Please refer to the AECL- number when requesting additional copies of this document

from

Scientific Document Distribution Office
Atomic Energy of Canada Limited
Chalk River, Ontario, Canada
K0J 1J0

Price: A

ISSN 0067 - 0367

Pour identifier les rapports individuels faisant partie de cette série nous avons assigné un numéro AECL- à chacun.

Veuillez faire mention du numéro AECL- si vous demandez d'autres exemplaires de ce rapport

au

Service de Distribution des Documents Officiels
L'Energie Atomique du Canada Limitée
Chalk River, Ontario, Canada
K0J 1J0

Prix: A

191-88